

$\bar{B} \rightarrow D^{(*)}\tau^-\bar{\nu}_\tau$ and Related Tauonic Topics at Belle

S. Hirose, For the Belle Collaboration

KMI, Nagoya University, Furo, Chikusa, Nagoya, Japan

The decays $\bar{B} \rightarrow D^{(*)}\tau^-\bar{\nu}_\tau$ are good probes to new physics beyond the Standard Model. The ratios of branching fractions $R(D^{(*)}) \equiv BF(\bar{B} \rightarrow D^{(*)}\tau^-\bar{\nu}_\tau)/BF(\bar{B} \rightarrow D^{(*)}\ell^-\bar{\nu}_\ell)$ (where $\ell^- = e^-, \mu^-$) measured by Belle, BaBar and LHCb show 3.9σ deviation from the SM expectations as of 2015. In 2016, the Belle collaboration has shown two new measurements for the $\bar{B} \rightarrow D^{(*)}\tau^-\bar{\nu}_\tau$ decay. These include the first application of the semileptonic tagging to the $R(D^*)$ measurement and the first measurement of the τ polarization using the hadronic τ decays. We also review the two measurements for $B^- \rightarrow \tau^-\bar{\nu}_\tau$ at Belle. Along with these results, compatibility with the type-II Two-Higgs-Doublet Model is discussed.

1 Introduction

Semileptonic and leptonic B meson decays containing a τ lepton in the final state are theoretically well-understood processes in the Standard Model (SM)¹. Owing to the existence of the two heavy fermions, a b quark and a τ lepton, they are sensitive to new physics (NP) beyond the SM if the NP has an enhanced coupling to the third-generation fermions. The decays $\bar{B} \rightarrow D^{(*)}\tau^-\bar{\nu}_\tau$ and $B^- \rightarrow \tau^-\bar{\nu}_\tau$ are these types of the B decays which have been experimentally investigated by the B -factory experiments, Belle and BaBar.^a LHCb has also demonstrated their capability of studying the $\bar{B} \rightarrow D^*\tau^-\bar{\nu}_\tau$ process at the Large Hadron Collider.

In this paper, we discuss the recent experimental results on $\bar{B} \rightarrow D^{(*)}\tau^-\bar{\nu}_\tau$ and $B^- \rightarrow \tau^-\bar{\nu}_\tau$ at the Belle experiment, where 8 GeV electrons and 3.5 GeV positrons are collided by the KEKB accelerator at the center-of-mass energy of 10.58 GeV. Pairs of B mesons are produced through the process $\Upsilon(4S) \rightarrow B\bar{B}$. The B meson decays are recorded by the Belle detector, which is a complex of six sub-detector systems².

2 Tagging Method

Due to multiple neutrinos in the final state, signal B mesons (B_{sig}) decaying into $D^{(*)}\tau^-\bar{\nu}_\tau$ or $\tau^-\bar{\nu}_\tau$ cannot be fully reconstructed. Exploiting the advantage of Belle that no particle except for two B mesons is produced in the $\Upsilon(4S)$ decay, we “tag” the B_{sig} candidate by reconstructing the counterpart B meson (B_{tag}) at first. The remaining particles in the event are then assigned to form a B_{sig} candidate.

There are two tagging methods applied to the $\bar{B} \rightarrow D^{(*)}\tau^-\bar{\nu}_\tau$ and $B^- \rightarrow \tau^-\bar{\nu}_\tau$ analyses. In the hadronic tagging method, B_{tag} is fully reconstructed from one of the hadronic decay modes. The four-momentum of B_{sig} is extracted by $p_{B_{\text{sig}}} = p_{e^+e^-} - p_{B_{\text{tag}}}$, where p 's are the four-momenta of the B_{sig} the e^+e^- beam and the B_{tag} , respectively. Belle has developed a hadronic tagging algorithm based on the NeuroBayes neural-network package³. This algorithm

^aThroughout this paper, the inclusion of the charge-conjugate mode is always implied.

uses 1104 decay chains in total, to achieve the highest possible B_{tag} reconstruction efficiency. The typical efficiency is around 0.2–0.3%.

The semileptonic tagging method uses the semileptonic decays such as $\bar{B} \rightarrow D^{(*)}\ell^- \bar{\nu}_\ell$. Although one neutrino in the semileptonic decay makes full reconstruction of B_{tag} impossible, the B_{tag} candidates are identified using the variable

$$\cos \theta_{B-D^{(*)}\ell} = \frac{2E_{\text{beam}}^* E_{D^{(*)}\ell}^* - m_B^2 c^4 - M_{D^{(*)}\ell}^2 c^4}{2|\vec{p}_B^*| |\vec{p}_{D^{(*)}\ell}^*| c^2}, \quad (1)$$

where E^* , \vec{p}^* and m (M) denote the energy, the momentum and the (reconstructed) mass, respectively, with the subscripts representing the e^+e^- beam, the B_{tag} and the $D^{(*)}\ell$ system. By requiring $\cos \theta_{B-D^{(*)}\ell}$ to lie in the physical region between -1 and 1 , correct B_{tag} candidates are obtained.

3 Experimental Results from Belle

3.1 Situation of $\bar{B} \rightarrow D^{(*)}\tau^- \bar{\nu}_\tau$ Studies before Winter 2016

The decays $\bar{B} \rightarrow D^{(*)}\tau^- \bar{\nu}_\tau$ have the relatively large branching fraction of $\mathcal{O}(1)\%$ among the B meson decay modes. Its three-body decay realizes to probe NP amplitudes using its kinematics such as the τ polarization, not only the branching fraction. To study the decays $\bar{B} \rightarrow D^{(*)}\tau^- \bar{\nu}_\tau$, the ratios of the branching fractions

$$R(D^{(*)}) \equiv \frac{BF(\bar{B} \rightarrow D^{(*)}\tau^- \bar{\nu}_\tau)}{BF(\bar{B} \rightarrow D^{(*)}\ell^- \bar{\nu}_\ell)} \quad (2)$$

are measured, where ℓ^- is an electron or a muon. In the ratios, the uncertainties in the Cabibbo-Kobayashi-Maskawa matrix element $|V_{cb}|$, the hadronic form factors and the experimental reconstruction efficiency are largely canceled. The SM predicts $R(D) = 0.300 \pm 0.008$ ⁴ and $R(D^*) = 0.252 \pm 0.003$ ⁵.

With the full data sample, Belle performed a measurement of $R(D^{(*)})$ using the hadronic tagging and the leptonic final state of the τ lepton⁶. The result was compatible with the SM expectation within 1.8σ . Including this result and the results from BaBar⁷ and LHCb⁸, the world-average $R(D)$ and $R(D^*)$ estimated by the heavy-flavor-averaging group (HFAG) were $0.391 \pm 0.041(\text{stat.}) \pm 0.028(\text{syst.})$ and $0.322 \pm 0.018(\text{stat.}) \pm 0.012(\text{syst.})$, respectively⁹. These were by 1.7 and 3.0σ away from the expectation based on the SM. The overall discrepancy reached 3.9σ .

3.2 New Measurements for $\bar{B} \rightarrow D^*\tau^- \bar{\nu}_\tau$

In 2016, Belle has shown the second and the third measurements for $\bar{B} \rightarrow D^*\tau^- \bar{\nu}_\tau$. The second one¹⁰ is based on the semileptonic tagging and provides an independent $R(D^*)$ measurement from the previous study. Due to less constraints of the semileptonic tagging on the B_{tag} kinematics, more background than the measurement with the hadronic tagging was predicted. Therefore only $R(D^*)$ has been measured from the $\bar{B}^0 \rightarrow D^{*+}\tau^- \bar{\nu}_\tau$ channel. For the B_{tag} decay, $\bar{B}^0 \rightarrow D^{*+}\ell^- \bar{\nu}_\ell$ has been chosen. Namely, the $\bar{B} \rightarrow D^*\tau^- \bar{\nu}_\tau$ (signal) event has $\bar{B}_{\text{sig}}^0 \rightarrow D^{*+}\tau^- \bar{\nu}_\tau$ and $B_{\text{tag}}^0 \rightarrow D^{*-}\ell^+ \nu_\ell$ while the $\bar{B} \rightarrow D^*\ell^- \bar{\nu}_\ell$ (normalization) event has $\bar{B}_{\text{sig}}^0 \rightarrow D^{*+}\ell^- \bar{\nu}_\ell$ and $B_{\text{tag}}^0 \rightarrow D^{*-}\ell^+ \nu_\ell$.

In this measurement, both signal and normalization events have the same final state: two D^* , two ℓ and a missing momentum. It is therefore important to consider how to separate the signal events from the normalization events. In one event, two values of $\cos \theta_{B-D^*\ell}$ are defined for each of the two B mesons. Due to three neutrinos, very often B_{sig} has $\cos \theta_{B-D^*\ell}$ significantly smaller than -1 . The smaller value of the two $\cos \theta_{B-D^*\ell}$ ($\cos \theta_{B-D^*\ell}^{\text{sig}}$) therefore provides efficient

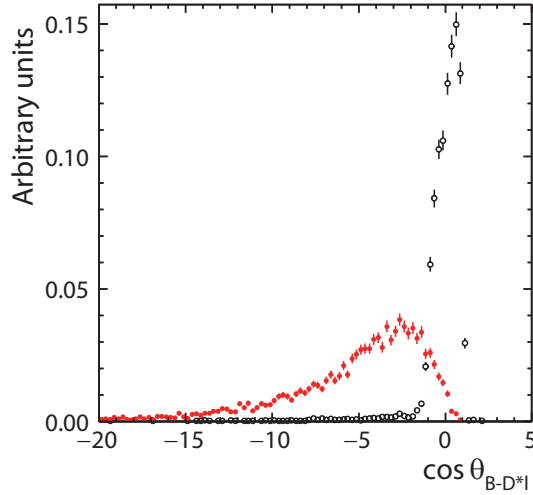


Figure 1 – Distribution of $\cos \theta_{B-D^* \ell}^{\text{sig}}$ for the signal events (solid red circles) and the normalization events (open black circles) from the Monte Carlo simulation.

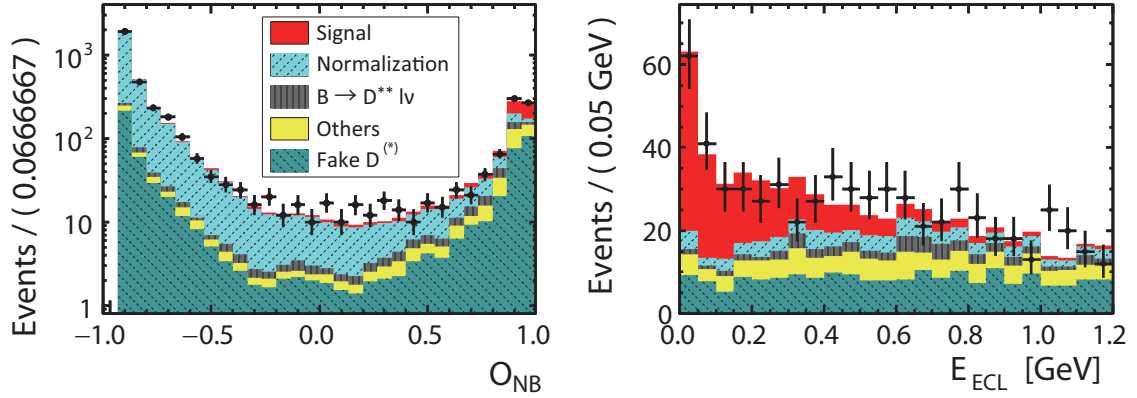


Figure 2 – Two-dimensional fit result. (left) Projection to O_{NB} . (right) Projection to E_{ECL} in the region $O_{\text{NB}} > 0.8$. For both panels, the black dots show the distribution from the experimental data while the solid colored histograms are the fitted probability density functions constructed from the Monte-Carlo simulation sample.

separation between the signal and the normalization events, as shown in Fig. 1¹⁰. Adding two more variables, a multi-variate analysis based on NeuroBayes is performed and the output classifier O_{NB} is constructed. Further details of the analysis are discussed in Ref.¹⁰.

Figure 2 shows the result of the two-dimensional fit using O_{NB} and E_{ECL} ¹⁰. The second variable E_{ECL} is the energy sum of the clusters in the electromagnetic calorimeter that are not used for the event reconstruction. Compared to the signal and the normalization events, other background events tend to have larger values of E_{ECL} due to additional photons from B meson decays. This measurement results in

$$R(D^*) = 0.302 \pm 0.030(\text{stat.}) \pm 0.011(\text{syst.}), \quad (3)$$

which is consistent with the SM within 1.6σ .

The third measurement¹² is based on the hadronic tagging and the hadronic τ decays $\tau^- \rightarrow \pi^- \nu_\tau$ and $\tau^- \rightarrow \rho^- \nu_\tau$. This choice of the τ final states allows a new $R(D^*)$ measurement independent of the result with $\tau^- \rightarrow \ell^- \bar{\nu}_\ell \nu_\tau$. Since the B_{sig} final state contains only hadrons, the main background component in this study arises from hadronic B decays. Their high-multiplicity

final states through complicated hadronization processes make both experimental measurements and theoretical predictions difficult. Estimation of the amount of hadronic B events in the signal region is thus one of the challenges. At the same time, this is an advantage as the background composition is different from the previous studies, where semileptonic B decays with the excited D mesons heavier than D^* are one of the major sources of the systematic uncertainty.

In addition to the new measurement of $R(D^*)$, the two-body τ decays allow a measurement of the τ polarization. It is defined by

$$P_\tau(D^*) \equiv \frac{\Gamma^+(D^*) - \Gamma^-(D^*)}{\Gamma^+(D^*) + \Gamma^-(D^*)}, \quad (4)$$

where $\Gamma^{+(-)}(D^*)$ is the decay rate for the τ lepton with a positive (negative) helicity state. The SM predicts $P_\tau(D^*) = -0.497 \pm 0.013$ ¹¹. This quantity is experimentally extracted from the differential decay rate

$$\frac{1}{\Gamma(D^*)} \frac{d\Gamma(D^*)}{d \cos \theta_{\text{hel}}} = \frac{1}{2} [1 + \alpha P_\tau(D^*) \cos \theta_{\text{hel}}], \quad (5)$$

where $\Gamma(D^*)$ and θ_{hel} denote the total decay rate and the angle of the τ -daughter meson momentum with respect to the direction opposite the virtual W boson^b momentum in the rest frame of τ . The coefficient α is represented by

$$\alpha = \begin{cases} 1 & \text{for } \tau^- \rightarrow \pi^- \nu_\tau \\ \frac{m_\tau^2 - 2m_\rho^2}{m_\tau^2 + 2m_\rho^2} & \text{for } \tau^- \rightarrow \rho^- \nu_\tau, \end{cases} \quad (6)$$

where m_τ and m_ρ are the masses of the τ lepton and the ρ meson, respectively.

Based on Eq. 5, $P_\tau(D^*)$ is related to the forward-backward asymmetry of the signal distribution:

$$P_\tau(D^*) = \frac{2 N_{\text{sig}}^{\text{F}} - N_{\text{sig}}^{\text{B}}}{\alpha N_{\text{sig}}^{\text{F}} + N_{\text{sig}}^{\text{B}}}, \quad (7)$$

where $N_{\text{sig}}^{\text{F(B)}}$ denotes the number of signal events in the region $\cos \theta_{\text{hel}} > (<) 0$.

Experimentally, the rest frame of τ cannot be exactly taken since the τ momentum is not completely determined. We instead use the rest frame of the $\tau \bar{\nu}_\tau$ system. In this frame shown in Fig. 3, the energy and the τ momentum are, respectively, determined by

$$E_\tau = \frac{q^2 + m_\tau^2/c^2}{2\sqrt{q^2}}, \quad (8)$$

$$|\vec{p}_\tau| = \frac{q^2 - m_\tau^2/c^2}{2\sqrt{q^2}}, \quad (9)$$

where $q^2 = p_{e^+e^-} - p_{B_{\text{tag}}} - p_{D^*}$ and p_{D^*} is the reconstructed four-momentum of D^* . Using E_τ and $|\vec{p}_\tau|$,

$$\cos \theta_{\tau d} = \frac{2E_\tau E_d - m_\tau^2 c^4 - m_d^2 c^4}{2|\vec{p}_\tau| |\vec{p}_d| c^2}, \quad (10)$$

is calculated, where E and \vec{p} are the energy and the three-momentum, respectively, of the τ lepton and the τ -daughter meson $d = \pi$ or ρ . Using the Lorentz transformation from this frame to the rest frame of τ , we obtain the equation

$$|\vec{p}_d^\tau| \cos \theta_{\text{hel}} = -\gamma |\vec{\beta}| E_d/c + \gamma |\vec{p}_d| \cos \theta_{\tau d}, \quad (11)$$

^bThere are two virtual W bosons in the $\bar{B} \rightarrow D^* \tau^- \bar{\nu}_\tau$ decay: one from the B meson decay and the other from the τ lepton decay. In this paper, W always denotes the virtual W boson from the B decay.

where

$$\gamma = \frac{E_\tau}{(m_\tau c^2)}, \quad (12)$$

$$|\vec{\beta}| = \frac{|\vec{p}_\tau|}{E_\tau}. \quad (13)$$

The τ -daughter momentum in the rest frame of τ is represented by

$$|\vec{p}_d^\tau| = \frac{m_\tau^2 - m_d^2}{2m_\tau}. \quad (14)$$

Solving Eq. 11, $\cos \theta_{\text{hel}}$ is obtained.

A fit is performed in two steps. First, the yield of the normalization events is measured using the missing-mass squared

$$M_{\text{miss}}^2 = (p_{e^+e^-} - p_{\text{tag}} - p_{D^*} - p_\ell)^2/c^2, \quad (15)$$

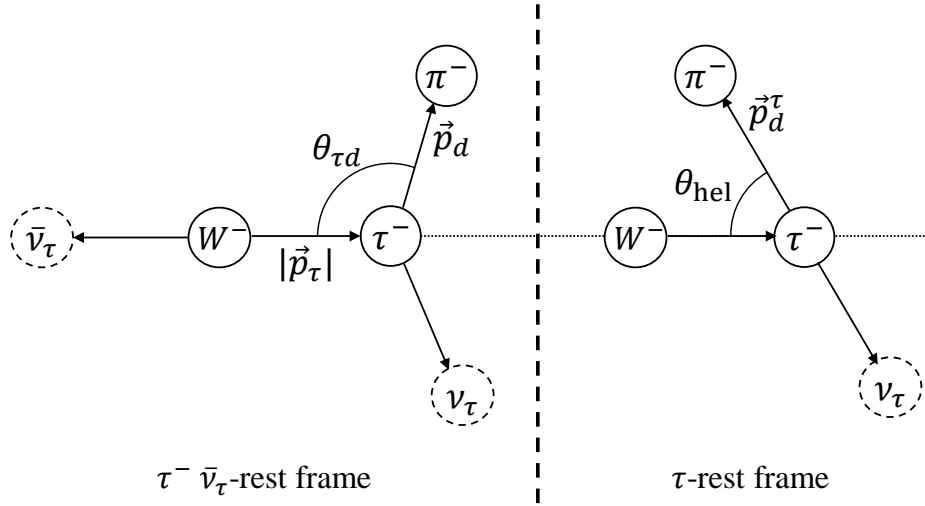


Figure 3 – Kinematics in the rest frame of the $\tau^- \bar{\nu}_\tau$ system and in the rest frame of τ .

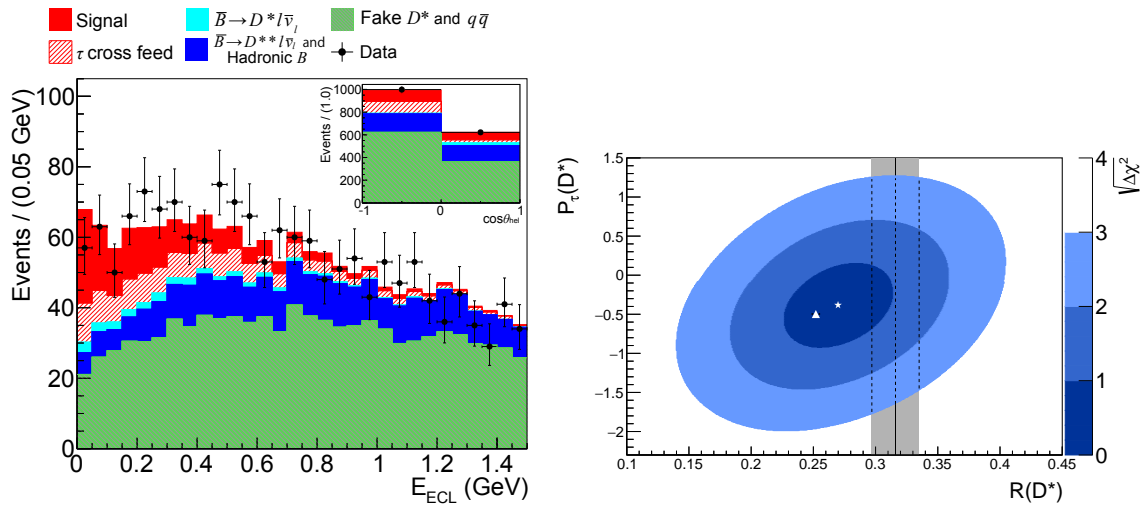


Figure 4 – Result from the $R(D^*)$ and $P_\tau(D^*)$ measurement using hadronic τ decays. (left) Fit result projected to the E_{ECL} and $\cos \theta_{\text{hel}}$ axes. (right) Comparison of our result (star for the best-fit value and 1σ , 2σ , 3σ contours) with the SM prediction (triangle). The shaded vertical band shows the world average without this result.

where p_ℓ denotes the four-momentum of ℓ and the other variables are defined previously. After determining the normalization yield, a two-dimensional fit is done using E_{ECL} and $\cos\theta_{\text{hel}}$, as shown in Fig. 4 (left)¹². The measurement results in

$$R(D^*) = 0.270 \pm 0.035(\text{stat.})_{-0.025}^{+0.028}(\text{syst.}), \quad (16)$$

$$P_\tau(D^*) = -0.38 \pm 0.51(\text{stat.})_{-0.61}^{+0.21}(\text{syst.}). \quad (17)$$

As illustrated in Fig. 4 (right)¹², the result is consistent with the SM expectations. The precision of $R(D^*)$ is 16%, which is comparable to 9–14% for the previous measurements with $\tau^- \rightarrow \ell^- \bar{\nu}_\ell \nu_\tau$. With the current statistics, the result excludes $P_\tau(D^*) > +0.5$ at 90% confidence level. This is the first measurement of $P_\tau(D^*)$ in $\bar{B} \rightarrow D^* \tau^- \bar{\nu}_\tau$.

Figure 5 illustrates the current situation for the $R(D^{(*)})$ studies summarized by HFAG⁹. The discrepancy between the world-average $R(D^{(*)})$ and the SM expectations remains at 3.9σ . This is because the new $R(D^*)$ results from Belle has made the world average closer to the SM but the $R(D^*)$ precision becomes better. The one $R(D)$ and three $R(D^*)$ results from Belle are compatible with the SM expectations within about 2σ while they tend to be consistently larger than the SM. Our results also agree with the other results by BaBar and LHCb within the current uncertainties. The discrepancy needs to be investigated further at the Belle II experiment, where 50 times more statistics will be available.

3.3 $B^- \rightarrow \tau^- \bar{\nu}_\tau$

The decay $B^- \rightarrow \tau^- \bar{\nu}_\tau$ is one of the purely-leptonic decays of the B meson. Due to the small value of the CKM matrix element $|V_{ub}|$, the branching fraction is suppressed to be $\mathcal{O}(10^{-4})$.

Belle has performed two measurements using the hadronic tagging and the semileptonic tagging^{13,14}. Figure 6 is the comparison of these results with the SM expectation from the preliminary estimation as of ICHEP 2016 by the CKM fitter group¹⁵. Their average is consistent with the SM expectation, and the significance is 4.0σ ¹⁴.

3.4 Discussion for the type-II Two-Higgs-Doublet Model

One of the prominent NP models possibly contributing to the decays $\bar{B} \rightarrow D^{(*)} \tau^- \bar{\nu}_\tau$ and $B^- \rightarrow \tau^- \bar{\nu}_\tau$ is the Two-Higgs-Doublet Model (2HDM) of type-II¹⁶. In this model, the charged Higgs boson H^\pm appears from the additional degrees of freedom in the Higgs doublets and has a large

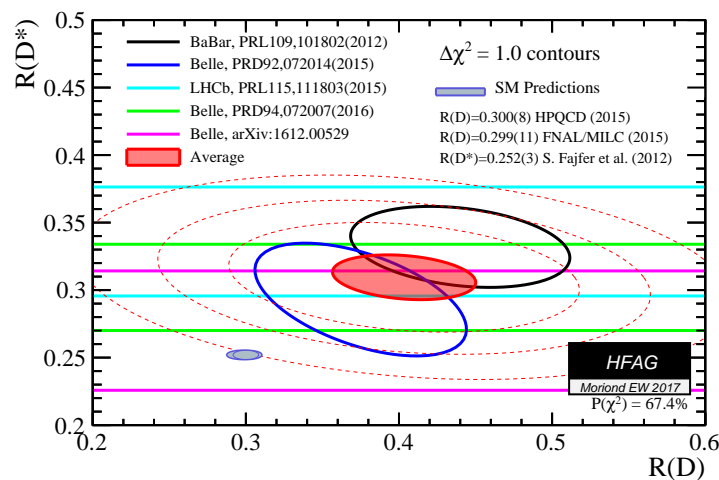


Figure 5 – Comparison of the experimental results on $R(D^{(*)})$ with the SM expectations.

coupling to b and τ . Based on the effective field theory, its contribution is represented by the Lagrangian^{11,17}

$$\mathcal{L}_{\text{eff}} = -2\sqrt{2}G_F V_{ib} \left(\mathcal{O}_{V_1} - m_b m_\tau \frac{\tan^2 \beta}{m_{H^\pm}} \mathcal{O}_{S_1} \right) \quad (i = u, c), \quad (18)$$

where G_F , m_b and m_{H^\pm} are the Fermi constant, the masses of the b quark and the charged Higgs, respectively. The parameter $\tan \beta$ denotes the ratio of the vacuum expectation values in the two Higgs doublets. The effective operators \mathcal{O}_{V_1} and \mathcal{O}_{S_1} corresponds to the SM- and the scalar-type interactions, respectively. See Ref.¹¹ for the explicit definition of these operators. According to this effective Lagrangian, the amplitude of the type-II 2HDM negatively interferes with the SM amplitude.

Belle has measured four observables for $\bar{B} \rightarrow D^{(*)} \tau^- \bar{\nu}_\tau$ and $B^- \rightarrow \tau^- \bar{\nu}_\tau$: $R(D)$, $R(D^*)$, $P_\tau(D^*)$ and the branching fraction for $B^- \rightarrow \tau^- \bar{\nu}_\tau$. Figure 7 compares our measurements with

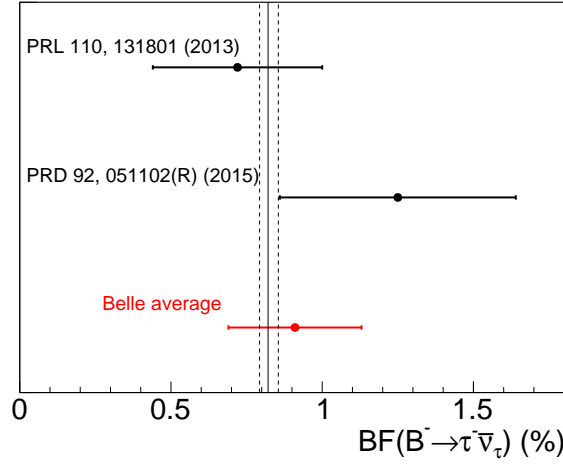


Figure 6 – Results from the $B^- \rightarrow \tau^- \bar{\nu}_\tau$ measurements at Belle. The vertical line shows the SM expectation with the $\pm 1\sigma$ region.

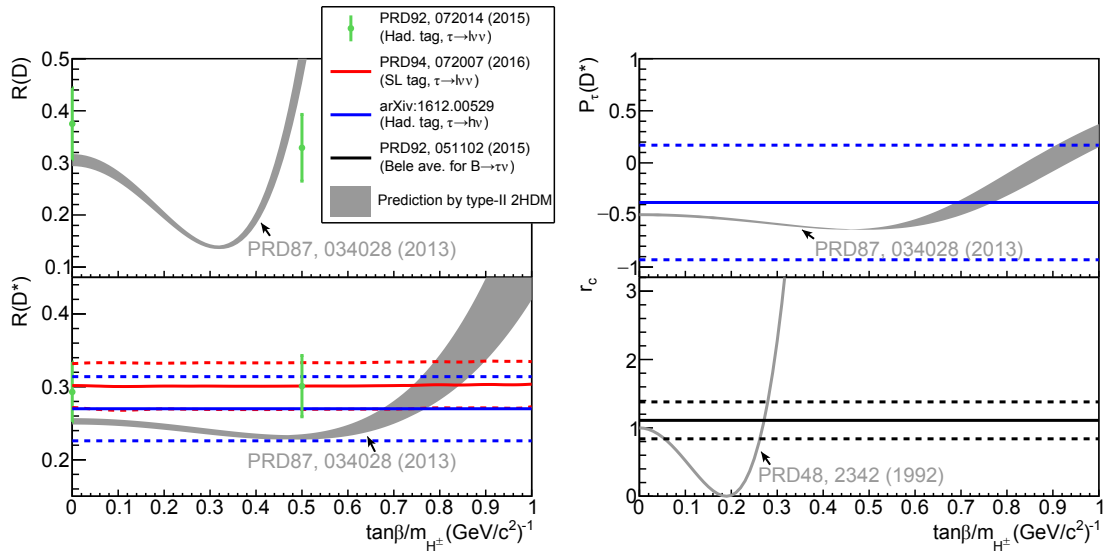


Figure 7 – Comparison between the measurements at Belle and the predictions based on the type-II 2HDM for $R(D)$ (top-left), $P_\tau(D^*)$ (top-right), $R(D^*)$ (bottom-left) and r_c (bottom-right). In the $R(D^*)$ and $P_\tau(D^*)$ measurement with the hadronic τ decays ($\tau^- \rightarrow h^- \nu_\tau$) and the r_c measurement, the efficiency is assumed to be uniform over $\tan \beta/m_{H^\pm}$. The other results include the efficiency correction as a function of $\tan \beta/m_{H^\pm}$.

the predictions from the type-II 2HDM. In this figure, r_c denotes the ratio of the measured or theoretically-expected branching fraction to the SM expectation. At the large $\tan\beta/m_{H^\pm}$ region, $R(D)$ and r_c favors different values of $\tan\beta/m_{H^\pm}$, and this region seems disfavored.

4 Conclusion

The decays $\bar{B} \rightarrow D^{(*)}\tau^-\bar{\nu}_\tau$ and $B^- \rightarrow \tau^-\bar{\nu}_\tau$ are interesting B decays in terms of their sensitivities to NP coupling to τ leptons, such as the charged Higgs in the type-II 2HDM. In 2016, Belle has shown two new $\bar{B} \rightarrow D^*\tau^-\bar{\nu}_\tau$ measurements. One of them is the first application of the semileptonic tagging to the $R(D^*)$ measurement. The second includes the first measurement of $R(D^*)$ using only hadronic τ decays and the first experimental study of $P_\tau(D^*)$.

We have discussed compatibility of our $\bar{B} \rightarrow D^{(*)}\tau^-\bar{\nu}_\tau$ and $B^- \rightarrow \tau^-\bar{\nu}_\tau$ measurements with the SM and the type-II 2HDM. All the observables measured by Belle are consistent with but higher than the SM expectations at the $2\text{-}\sigma$ level. For the type-II 2HDM, our results seem to favor the region with small values of $\tan\beta/m_{H^\pm}$.

The world-average $R(D^{(*)})$ including measurements at BaBar and LHCb shows the $3.9\text{-}\sigma$ discrepancy from the SM expectations. With the current precision at Belle, our result is consistent both with the results from these experiments and the SM expectations within about 2σ . This is an important topic to be further investigated with a high precision at Belle II.

Acknowledgments

This work was partially supported by JSPS Grant-in-Aid for Scientific Research (S) ‘‘Proving New Physics with Tau-Lepton’’ (No. 26220706).

References

1. For example, D.S. Hwang and D.-W. Kim, E. Phys. J. C **14**, 271 (2000).
2. A. Abashian *et al.* (Belle Collaboration), Nucl. Instr. and Meth. A **479**, 117 (2002); also see the detector section in J. Brodzicka *et al.*, Prog. Theor. Exp. Phys. **2012**, 04D001 (2012).
3. M. Feindt *et al.*, Nucl. Instr. and Meth. A **654**, 432 (2011).
4. H. Na *et al.* (HPQCD Collaboration), Phys. Rev. D **92**, 054510 (2015).
5. S. Fajfer, J.F. Kamenik and I. Nišandžić, Phys. Rev. D **85**, 094025 (2012).
6. M. Huschle *et al.* (Belle Collaboration), Phys. Rev. D **92**, 072014 (2015).
7. J.P. Lees *et al.* (BaBar Collaboration), Phys. Rev. Lett. **109**, 101802 (2012).
8. R. Aaij *et al.* (LHCb Collaboration), Phys. Rev. Lett. **115**, 111803 (2015).
9. Y. Amhis *et al.* (Heavy Flavor Averaging Group), arXiv:1612.07233 (2016) and online update at <http://www.slac.stanford.edu/xorg/hfag/>.
10. Y. Sato *et al.* (Belle Collaboration), Phys. Rev. D **94**, 072007 (2016).
11. M. Tanaka and R. Watanabe, Phys. Rev. D **87**, 034028 (2013).
12. S. Hirose *et al.* (Belle Collaboration), arXiv:1612.00529, accepted by Phys. Rev. Lett.
13. K. Hara *et al.* (Belle Collaboration), Phys. Rev. Lett. **110**, 131801 (2013).
14. B. Kronenbitter *et al.* (Belle Collaboration), Phys. Rev. D **92**, 051102(R) (2015).
15. CKM fitter: <http://ckmfitter.in2p3.fr/>
16. J.F. Gunion, H.E. Haber, G.L. Kane and S. Dawson, Front. Phys. **80**, 1 (2000).
17. W.-S. Hou, Phys. Rev. D **48**, 2342 (1992).